AMERICAN SOCIETY FOR MICROBIOLOGY | Journal of Virology®

TRANSFORMATION AND ONCOGENESIS

Expression Ratios of the Antiapoptotic BCL2 Family Members Dictate the Selective Addiction of Kaposi's Sarcoma-Associated Herpesvirus-Transformed Primary Effusion Lymphoma Cell Lines to MCL1

Daniel Dunham,[a,b,c] Prasanth Viswanathan,[a,b,c] Jackson Gill,[d] Mark Manzano[a,b,c]

[a]Department of Microbiology and Immunology, University of Arkansas for Medical Sciences, Little Rock, Arkansas, USA
[b]Center for Microbial Pathogenesis and Host Inflammatory Responses, University of Arkansas for Medical Sciences, Little Rock, Arkansas, USA
[c]Winthrop P. Rockefeller Cancer Institute, University of Arkansas for Medical Sciences, Little Rock, Arkansas, USA
[d]Department of Biological Sciences, Henderson State University, Arkadelphia, Arkansas, USA

Daniel Dunham and Prasanth Viswanathan equally contributed to this article. Author order was determined based on project initiation.

ABSTRACT Kaposi's sarcoma-associated herpesvirus (KSHV) causes several malignancies in people living with HIV, including primary effusion lymphoma (PEL). PEL cell lines exhibit oncogene addictions to both viral and cellular genes. Using CRISPR screens, we previously identified cellular oncogene addictions in PEL cell lines, including MCL1. MCL1 is a member of the BCL2 family, which functions to prevent intrinsic apoptosis and has been implicated in several cancers. Despite the overlapping functions of the BCL2 family members, PEL cells are dependent only on MCL1, suggesting that MCL1 may have nonredundant functions. To investigate why PEL cells exhibit selective addiction to MCL1, we inactivated the intrinsic apoptosis pathway by engineering BAX/BAK1 double knockout cells. In this context, PEL cells become resistant to MCL1 knockdown or MCL1 inactivation by the MCL1 inhibitor S63845, indicating that the main function of MCL1 in PEL cells is to prevent BAX/BAK1-mediated apoptosis. The selective requirement to MCL1 is due to MCL1 being expressed in excess over the BCL2 family. Ectopic expression of several BCL2 family proteins, as well as the KSHV BCL2 homolog, significantly decreased basal caspase 3/7 activity and buffered against staurosporine-induced apoptosis. Finally, overexpressed BCL2 family members can functionally substitute for MCL1, when it is inhibited by S63845. Together, our data indicate that the expression levels of the BCL2 family likely explain why PEL tumor cells are highly addicted to MCL1. Importantly, our results suggest that caution should be taken when considering MCL1 inhibitors as a monotherapy regimen for PEL because resistance can develop easily.

IMPORTANCE Primary effusion lymphoma (PEL) is caused by Kaposi's sarcoma-associated herpesvirus. We showed previously that PEL cell lines require the antiapoptotic protein MCL1 for survival but not the other BCL2 family proteins. This selective dependence on MCL1 is unexpected as the BCL2 family functions similarly in preventing intrinsic apoptosis. Recently, new roles for MCL1 not shared with the BCL2 family have emerged. Here, we show that noncanonical functions of MCL1 are unlikely essential. Instead, MCL1 functions mainly to prevent apoptosis. The specific requirement to MCL1 is due to MCL1 being expressed in excess over the BCL2 family. Consistent with this model, shifting these expression ratios changes the requirement away from MCL1 and toward the dominant BCL2 family gene. Together, our results indicate that although MCL1 is an attractive chemotherapeutic target to treat PEL, careful consideration must be taken, as resistance to MCL1-specific inhibitors easily develops through BCL2 family overexpression.

Editor Jae U. Jung, Lerner Research Institute, Cleveland Clinic

Address correspondence to Mark Manzano, mmanzano@uams.edu.

The authors declare no conflict of interest.

Received 5 September 2022
Accepted 10 November 2022
Published 23 November 2022

KEYWORDS KSHV, primary effusion lymphoma, MCL1, cell death, apoptosis, BCL2, vBCL2, S63845

Kaposi's sarcoma-associated herpesvirus (KSHV) establishes lifelong latency in B cells. While KSHV infections are often asymptomatic, they can develop into lymphoproliferative disorders, such as multicentric Castleman disease and primary effusion lymphoma (PEL) in people living with HIV (1). PEL is a monoclonal B cell malignancy often found as effusions in body cavities (2). Patients treated with modified etoposide, vincristine, and doxorubicin with cyclophosphamide and prednisone (EPOCH) have a median survival time of 22 months and a 3-year survival rate of 47% (3). To date, no cancer-specific treatment is available for PEL.

PEL cell lines exhibit gene expression profiles closest to plasma cells (4–6) with elevated levels of key plasma cell-associated transcripts, such as the master transcription factor interferon regulator factor 4 (IRF4) and genes involved in the unfolded protein response and endoplasmic reticulum stress (ER) pathways (4, 7). The majority of PEL tumors (~80%) are also coinfected with the related gammaherpesvirus Epstein-Barr virus (EBV). The presence of EBV appears to improve prognosis in patients (3). Genetic analyses of PEL tumors do not show mutations or translocations found in other hematological malignancies, such as *TP53*, *MYC*, *BCL2*, or *BCL6* (2, 8–10), although alterations in fragile site tumor suppressors have been reported (11). Instead, the defining feature of PEL is that all tumor cells are latently infected with KSHV. The latent virus constitutively expresses only a narrow subset of latency genes and at least 20 mature viral microRNAs.

It is thought that constitutive expression of the KSHV latency genes drives the transformation of PEL. Knockdown of the viral cyclin, viral FLICE inhibitory protein, viral interferon regulatory factors 1 to 3 (vIRF1 to 3), or viral interleukin 6 all led to a decrease in the survival of PEL cells in culture (12–16). These latency genes regulate cellular networks to constitutively activate pathways necessary to support the survival and proliferation of these infected cells. This process creates "oncogenic dependencies or addictions" to cellular genes because tumor cells rely on the continuous signaling of these pathways. For instance, addictions to several oncogenes have been reported in PEL cell lines, including the constitutive NF-κB signaling, phosphatidylinositol-3-kinase-mTOR signaling, gp130-STAT3 signaling, high expression of the p53 inhibitor MDM2 and the IRF4 transcription factor, and c-Myc stabilization (9, 17–25).

We recently performed genome-wide CRISPR knockout (KO) screens to comprehensively identify human oncogenic addictions or cellular genes that are required for the survival and/or proliferation of PEL cell lines (26). Our study confirmed the addictions to well-described pathways above. Importantly, we uncovered new dependencies that are consistently required in eight different PEL cell lines which included genes that are commonly essential regardless of cell type and genes that are strongly selective. We identify a strong addiction to the myeloid cell leukemia-1 gene (MCL1). MCL1 belongs to the BCL2 gene family, of which there are six members, as follows: MCL1, BCL2, BCL-xL (encoded by *BCL2L1*), BCL-W (encoded by *BCL2L2*), A1 (encoded by *BCL2A1*), or Diva (encoded by *BCL2L10*). The BCL2 family functions to inhibit intrinsic apoptosis. In healthy cells, monomers of the apoptotic effector BAX or BAK1 are sequestered on the mitochondrial outer membrane (MOM) by the BCL2 family proteins (Fig. 1A). When intrinsic apoptosis is initiated, proapoptotic BH3-only proteins (e.g., PUMA and NOXA) bind to the BCL2 family proteins to release the BAX/BAK1 monomers. The monomeric effectors oligomerize to form pores in the MOM and trigger an apoptotic cascade (27). MOM permeabilization is often considered the "point of no return" for cell death.

Although the BCL2 family members share the same function in BAX/BAK1 sequestration, PEL cell lines appear to be addicted only to MCL1 (Fig. 1B). In recent years, new roles beyond apoptosis have been described for MCL1. MCL1 has been implicated in mitochondrial fusion, respiration, fatty acid oxidation, and autophagy (28–30). In this study, we investigate the basis for why KSHV-transformed PEL cell lines exhibit

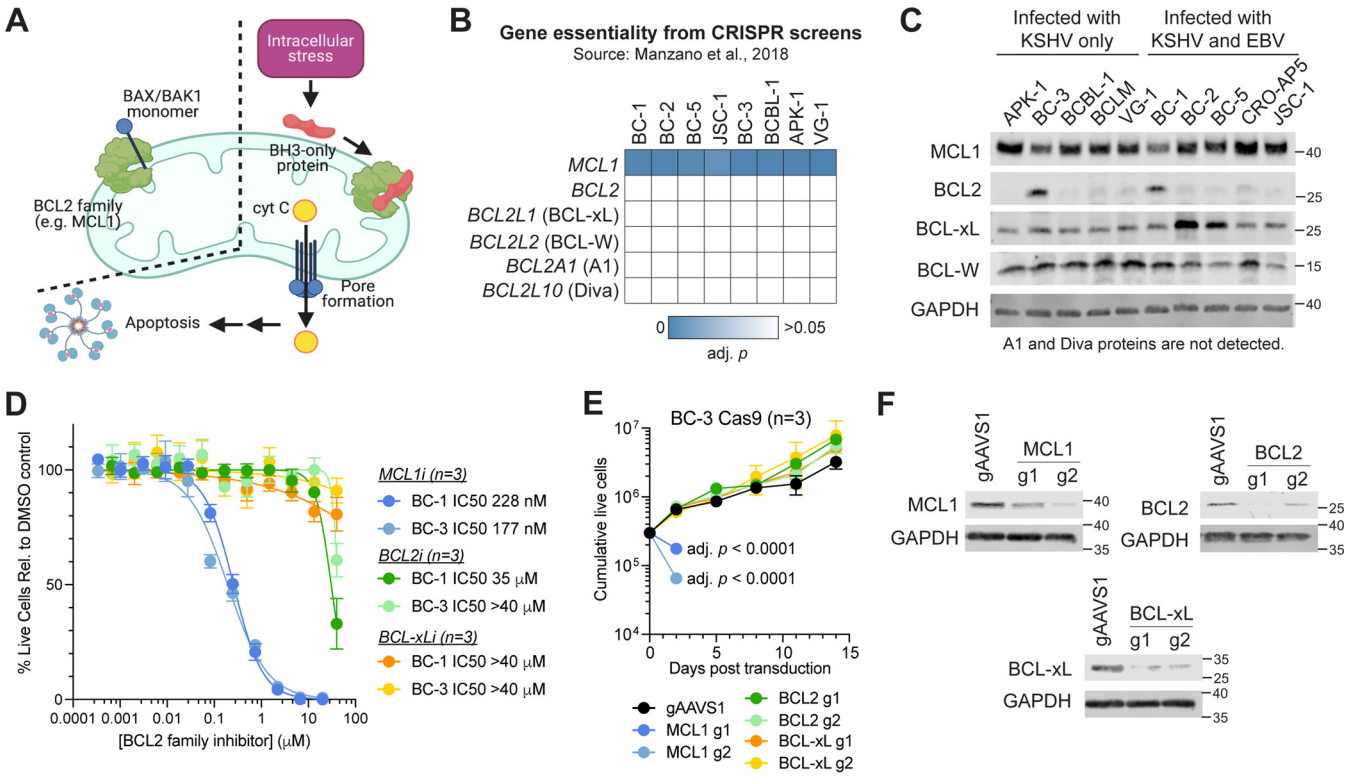

FIG 1 (A) The BCL2 family proteins (including MCL1) block intrinsic apoptosis by sequestering activated BAX or BAK1 monomers on the outer membrane of the mitochondria. During intrinsic apoptosis, proapoptotic BH3-only proteins inactivate the BCL2 family proteins and release the BAX/BAK1 monomers. Free monomers assemble to create mitochondrial pores and release cytochrome c to initiate the apoptotic cascade in the cytoplasm. (B) Only gRNAs targeting MCL1 among the BCL2 family are significantly depleted in all PEL cell lines that were screened previously (26). (C) Western blots of the different BCL2 family proteins in a panel of PEL cell lines infected with KSHV only or coinfected by KSHV and EBV. A1 and Diva proteins are not detected. (D) Dose-response curves of BC-1 and BC-3 cells treated with MCL1i, BCL2i, or BCL-xLi. (E) Cumulative live cell plot of BC-3 Cas9 cells transduced with lentiviruses expressing gRNAs against AAVS1, MCL1, BCL2, or BCL-xL. MCL1 g1 and g2 cells were not counted beyond day 2 because of low numbers of live cells. Statistical differences were calculated using two-way analysis of variance (ANOVA) with Dunnett's multiple-comparison test (n = 3). (F) Representative Western blots of MCL1, BCL2, BCL-xL, or GAPDH at day 2 from E. Samples targeting MCL1 and BCL-xL were run on the same gel flanking the same gAAVS1 control.

selective dependence on only MCL1 among the BCL2 gene family. Here, we show that the main essential function of MCL1 in PEL cells is to block intrinsic apoptosis and that noncanonical roles are unlikely. PEL cell lines likely depend on MCL1 because it is expressed at 15- to 60-fold higher levels than the other BCL2 family members. Altering the expression ratios by overexpression of the other BCL2-related proteins, including the KSHV BCL2 homolog, rescues cells from intrinsic apoptosis induced by an inhibitor of MCL1. This result suggests that endogenous expression levels of the BCL2 proteins determine the selective addiction to MCL1 in KSHV-transformed PEL cell lines.

RESULTS

Primary effusion lymphoma cells are selectively addicted to MCL1. We previously identified host gene addictions of KSHV-transformed PEL cell lines using genome-wide CRISPR screens (26). Our work showed that these tumor cells require high expression of the oncogene MCL1 for survival. Although the BCL2 family proteins share similar roles in preventing intrinsic apoptosis (Fig. 1A), none of the other BCL2 family genes scored in our CRISPR screens (Fig. 1B). To exclude the possibility that the selective addiction to MCL1 is due to the absence of the other BCL2 family proteins, we performed Western blotting for endogenously expressed BCL2, BCL-xL, BCL-W, A1, Diva, or MCL1 proteins in a panel of PEL cell lines (Fig. 1C). This panel included five cell lines that are coinfected with EBV (BC-1, BC-2, BC-5, CRO-AP5, and JSC-1) and five that are only infected with KSHV (APK-1, BC-3, BCBL-1, BCLM, and VG-1). Our immunoblots show that PEL cell lines uniformly express BCL-xL, BCL-W, and MCL1. In contrast, BCL2

expression is detectable only in BC-1 and BC-3 cells, while we do not detect A1 or Diva in any of the cell lines. Similar expression patterns of MCL1, BCL2, and BCL-xL were recently reported in additional PEL cell lines (31).

To confirm the selective dependence of PEL cell lines to MCL1, we treated BC-1 or BC-3 cells with small molecule inhibitors that are specific for MCL1 (S63845, "MCL1i"), BCL2 (ABT-199/venetoclax, "BCL2i"), or BCL-xL (WEHI-539, "BCL-xLi"). These inhibitors are not expected to cross-inhibit the other BCL2 members. No BCL-W-specific inhibitors have been developed to date. Consistent with our previous work (26), BC-1 and BC-3 cells are sensitive to MCL1i with an estimated half maximal inhibitory concentration (IC_{50}) of 177 to 228 nM (Fig. 1D). In contrast, both cell lines are resistant to BCL2i and BCL-xLi. These results are consistent with a study showing that PEL cell lines are sensitive to another MCL1i inhibitor, AZD-5991, but are resistant to the dual BCL2/BCL-xL inhibitor ABT-263 (31).

To further demonstrate that PEL cell lines selectively depend on MCL1 but not the other BCL2 family members, we targeted the endogenously expressed MCL1, BCL2, or BCL-xL for pooled CRISPR knockout (KO) in BC-3 Cas9 cell lines. Our efforts to target BCL-W for CRISPR KO were unsuccessful. Similar to what we observed previously (26), pooled MCL1 KO cells significantly decreased cell viability by 70 to 90% as early as 2 days after the transduction of lentivirus-encoding MCL1 guide RNAs (gRNAs) (Fig. 1E and F). In contrast, pooled BCL2 and BCL-xL KO cells had similar viability compared with a negative control which targets the *AAVS1* safe harbor locus (gAAVS1) for 2 weeks. In summary, our data indicate that PEL cell lines express the other BCL2 family proteins but are selectively addicted to MCL1.

BAX/BAK1 double knockout (DKO) cell lines. Roles beyond inhibiting apoptosis have emerged for MCL1, including facilitating mitochondrial respiration and fatty acid oxidation (28–30). We thus explored whether MCL1 may have critical noncanonical functions in PEL cells that necessitate MCL1 expression but not the expression of other BCL2 proteins, in addition to its canonical role in inhibiting intrinsic apoptosis.

Loss-of-function studies on the noncanonical roles of MCL1 pose a technical hurdle because they are confounded by effects from cell death. To address this issue, we derived clonal BAX and BAK1 double knockout (DKO) cell lines from BC-1 (KSHV+EBV+) and BC-3 (KSHV+) cells (Fig. 2A and B). This process inactivates the intrinsic apoptosis pathway since pore formation by BAX or BAK1 is considered the necessary step to irreversibly initiate intrinsic apoptosis (Fig. 1A).

We tested whether the DKO mutations successfully inactivate the intrinsic apoptotic pathway after treatment with staurosporine. Staurosporine induces intrinsic apoptosis by broadly inhibiting protein kinases. In parallel, we also tested the sensitivities of the DKO cells to different antibiotics. Dose-response curves for these inhibitors show that DKO cell clones are substantially resistant to treatment with staurosporine but remain sensitive to the antibiotics puromycin, blasticidin, zeocin, and hygromycin (Fig. 2C to G). Our data thus confirm that our DKO cell clones successfully inactivate the intrinsic apoptotic pathway but not other cell death mechanisms.

Knockout of BAX and BAK1 eliminates the dependency of PEL cells to MCL1. We used the BC-1 and BC-3 DKO cell clones to investigate their dependency on MCL1. If the inactivation of MCL1 continues to affect the viability of DKO cells, it would suggest that MCL1 has an essential role in PEL that is independent of intrinsic apoptosis. In contrast, if the DKO cells are unaffected by MCL1 inhibition, then the main essential function of MCL1 is to inhibit BAX/BAK1-mediated cell death.

We therefore treated BC-1 and BC-3 wild-type (WT) and DKO cells with increasing doses of the MCL1 inhibitor S63845 (MCL1i) (32). Consistent with our previous work (26) and Fig. 1D, WT BC-1 and BC-3 cells are sensitive to MCL1i (Fig. 3A). However, both DKO cell clones were resistant to MCL1i and viable even at the maximum dose used (20 μM).

To confirm whether MCL1i induces apoptosis in PEL cells, we treated the WT and DKO cells with a sublethal dose of MCL1i (100 nM) overnight and measured apoptotic markers using annexin V/7-aminoactinomycin D (7-AAD) staining and caspase 3/7

A

Locus	BC-1 #28 *BAX*$^{-/-}$*BAK1*$^{-/-}$	BC-3 #12 *BAX*$^{-/-}$*BAK1*$^{-/-}$
BAX	Allele 1: Ex3 +1, Δ3, T-G Allele 2: Ex3 Δ115 band	No wt band by PCR Ex3 Δ115 band only
BAK1	Allele 1: Rearranged Ex3-4 Allele 2: Ex3-4 Δ249	No wt band by PCR Ex3 ins115, Ex4 Δ58

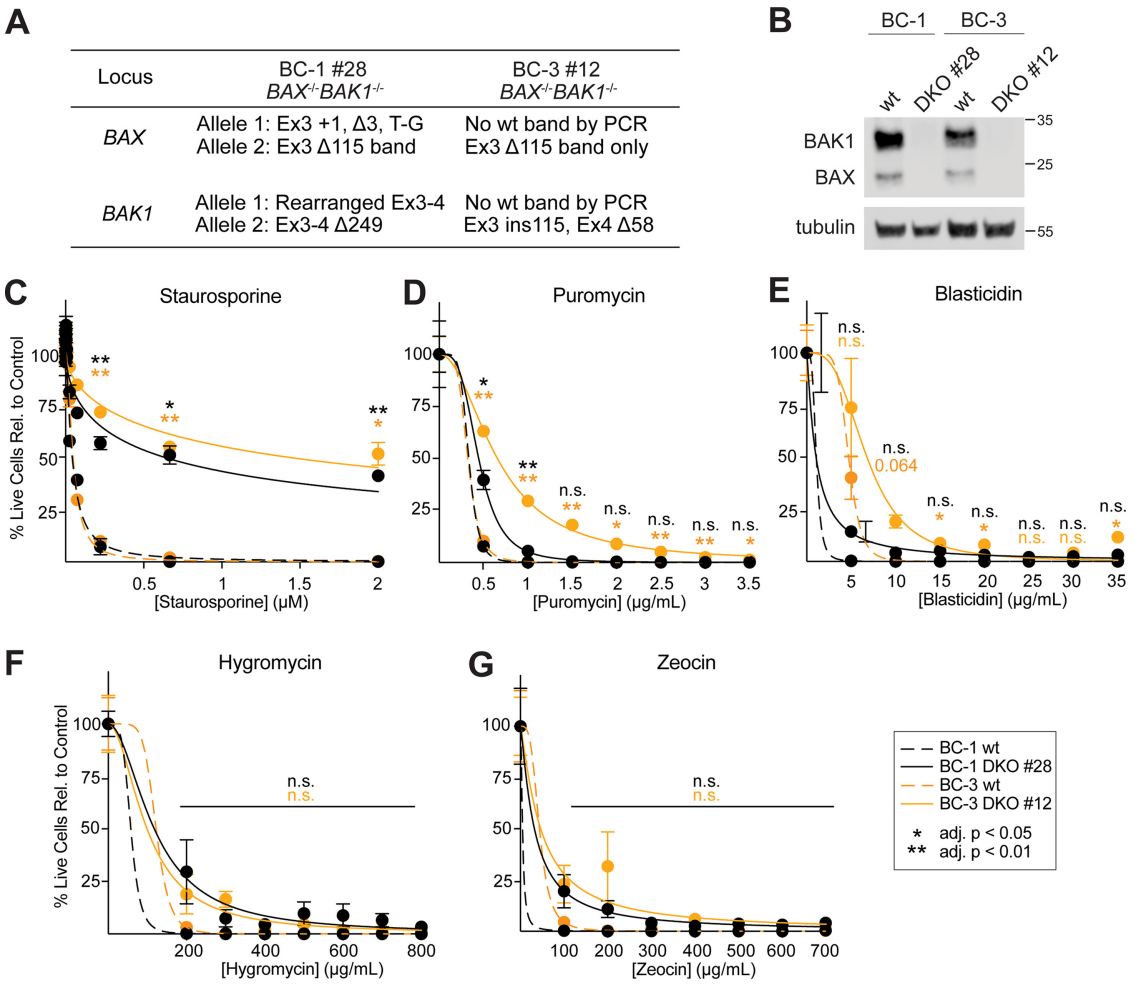

FIG 2 (A) Summary of CRISPR edits in BC-1 BAX/BAK1 double knockout (DKO) clone 28 and BC-3 DKO clone 12. (B) Western blots for BAX, BAK1, and tubulin proteins of WT or DKO cells in A. (C to G) Dose-response curves of BC-1 or BC-3 cells with BAX/BAK1 wild-type or DKO background upon exposure to different inducers of cell death, as follows: staurosporine (C), puromycin (D), blasticidin (E), hygromycin (F), or zeocin (G). Statistical differences were calculated using two-way ANOVA with Tukey's multiple comparison *post hoc* test (n = 3). Adjusted P values reflect *post hoc* comparisons between the responses of the WT cell line compared with the DKO cell line at the specific time point. Error bars, standard error of mean. n.s., not significant.

luciferase assay. We also included a sublethal dose of staurosporine (20 nM) treatment as a positive control. Exposure to MCL1i or staurosporine of BC-1 or BC-3 WT cells decreased live cells between 5 and 40% compared with the dimethyl sulfoxide (DMSO) control (Fig. 3B). This decrease is accompanied by a proportional increase in cells undergoing early and late apoptosis (Fig. 3B) as well as an increase in caspase 3/7 activities (Fig. 3C). In contrast, all of these markers of programmed cell death are completely rescued in BC-1 and BC-3 DKO cells. Thus, apoptotic cell death induced by the pharmacological inhibition of MCL1 is prevented by genetically ablating BAX and BAK1.

Since MCL1i was specifically designed to bind to the BH3-binding groove of MCL1 (32), it is possible that MCL1i induces cell death by inhibiting the antiapoptotic role of MCL1 without affecting putative noncanonical functions. We therefore targeted MCL1 for RNA interference (RNAi) knockdown in both BC-3 WT and DKO cells using a doxycycline (DOX)-inducible lentiviral short hairpin RNA (shRNA). Total MCL1 protein was reduced by ~70% by quantitative Western blot in both WT and DKO cells using the sh2MCL1 construct after DOX addition (Fig. 4A). This result is not seen in the absence of DOX nor in a negative-control shRNA construct targeting the *Renilla* luciferase (33). Similar to our previous work (26), MCL1 knockdown led to a significant decrease in the

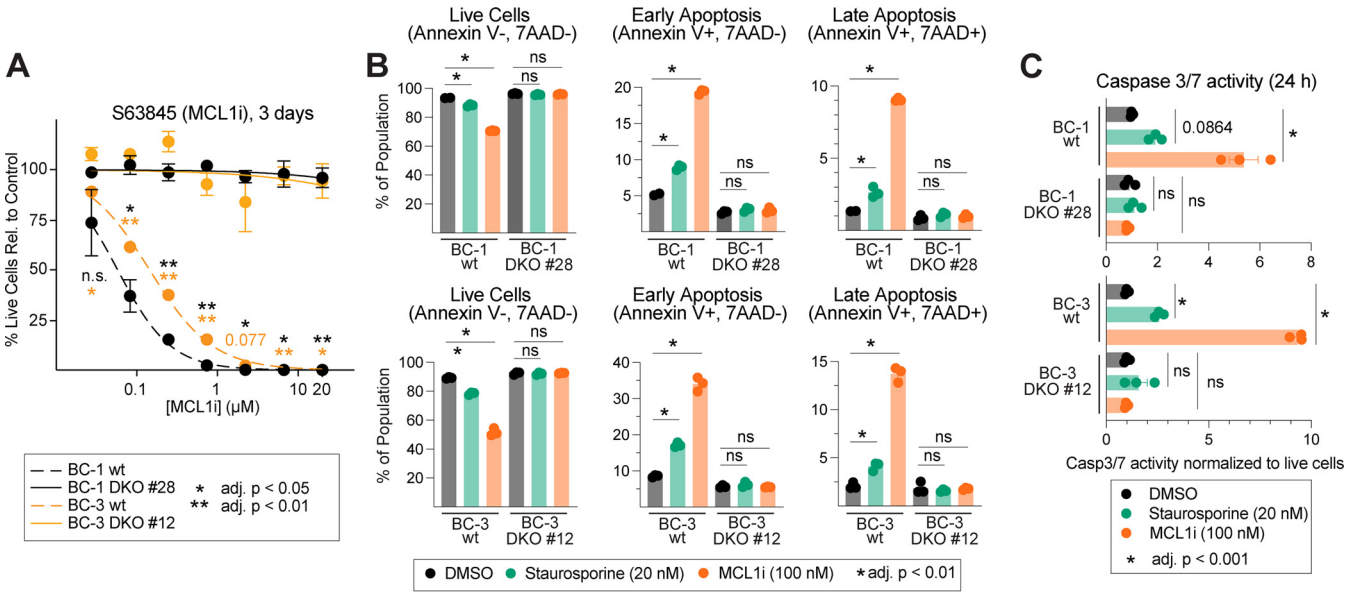

FIG 3 (A) MCL1i dose-response curves of BC-1 or BC-3 cells with BAX/BAK1 WT or DKO background. (B) Distribution of live, early apoptotic or late apoptotic cell populations of BC-1 and BC-3 WT or DKO cells after an overnight treatment of 100 nM MCL1i or 20 nM staurosporine as determined by annexin V/7-AAD staining. (C) In parallel, caspase 3/7 activities were measured using a luciferase assay from cells in B. Statistical differences were calculated using one-way ANOVA with Tukey's multiple-comparison test (n = 3). Error bars, standard error of mean. ns, not significant.

total number of live cells in BC-3 WT cells as early as 2 days after DOX treatment (Fig. 4B, dotted red line). This decrease is accompanied by an ~7-fold increase in caspase 3/7 activity (Fig. 4C). In contrast, MCL1 knockdown in BC-3 DKO cells did not substantially affect viability even after 12 days of DOX treatment (Fig. 4B, dotted purple line) nor induce caspase 3/7 activity (Fig. 4C). We note the efficiency of MCL1 knockdown is sustained at this time point as evidenced by reduced MCL1 protein (Fig. 4A, bottom). Taken together, our results from the MCL1i treatment or shRNA knockdown of the DKO cells suggest that the essential function of MCL1 in PEL cell lines is to prevent intrinsic apoptosis.

Overexpression of BCL2 proteins in PEL cell lines. Our results thus far indicate that the main role of MCL1 in PEL cell lines is to inhibit cell death. However, this result does not address why we observe a selective addiction to MCL1 in our CRISPR screens despite coexpression of functionally similar BCL2 proteins. Because a minimum number of prosurvival BCL2 family protein molecules is required to successfully neutralize BAX/BAK1 monomers and prevent pore formation, we hypothesized that the expression ratios of the BCL2 family directly influence the addiction to MCL1. Although we detected BCL-xL and BCL-W proteins in all PEL cell lines and BCL2 in BC-1 and BC-3 (Fig. 1C), Western blotting does not allow for relative quantification between different proteins even in the same sample. We therefore reanalyzed publicly available mRNA sequencing (mRNA-seq) data sets from different PEL cell lines, including other B cell malignancies, to determine the abundance of the BCL2 family transcripts (34). As seen in Fig. 5A, endogenous MCL1 is the most highly expressed BCL2 family gene in all six PEL cell lines. In contrast, BCL2, BCL-xL, and BCL-W mRNA levels are expressed only modestly (15- to 60-fold less than that of MCL1) while A1 and Diva mRNAs are not detected. This expression profile reflects the degree of depletion of gRNAs from the CRISPR screens (Fig. 1B), consistent with the model in which expression ratios of the BCL2 family may influence the selective addiction to MCL1. Notably, these ratios and magnitude of MCL1 expression in PEL cell lines are similar to what is seen in multiple myeloma cell lines which are also considered to be plasma cell-like. This finding is consistent with previous reports demonstrating that the PEL and multiple myeloma cell lines have similar gene expression profiles (4–6). These expression patterns of the BCL2 family genes are distinct from those observed in other B cell malignancies that

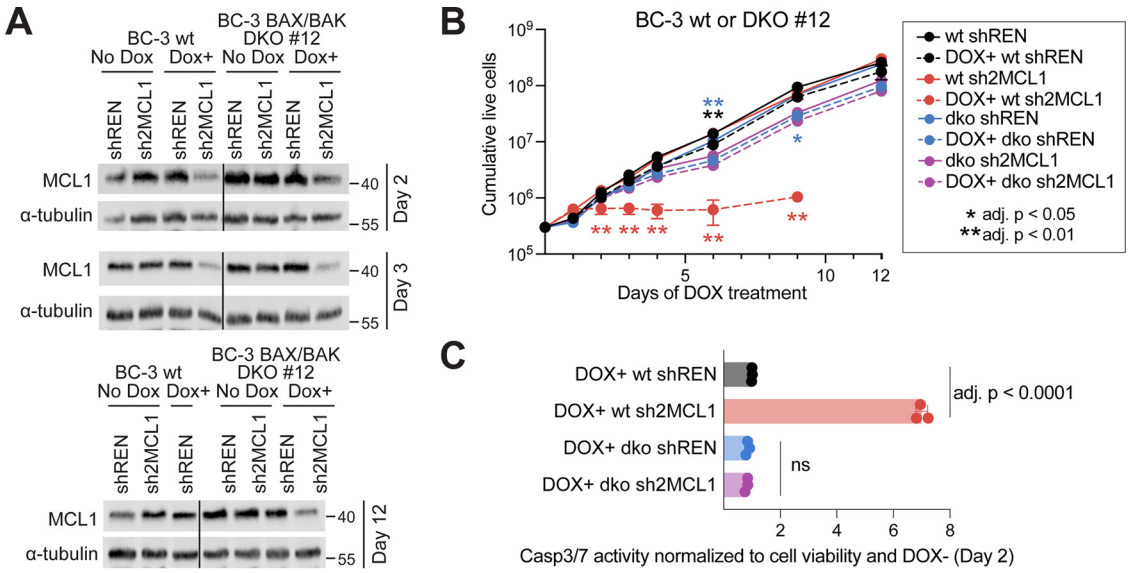

FIG 4 (A) Western blots for total MCL1 in BC-3 BAX/BAK WT or DKO #12 cells transduced with lentiviruses expressing a doxycycline (DOX)-inducible shRNA against *Renilla* luciferase or MCL1. Shown are samples taken after 2, 3, or 12 days of DOX treatment (1 μg/mL). (B) Cumulative live-cell count of BC-3 cells upon DOX treatment (dotted lines). Cell counts were terminated for DOX-treated BC-3 WT cells with sh2MCL1 (dotted red line) at day 9 of DOX treatment due to a significant amount of cell death. Statistical differences were calculated using one- or two-way ANOVA with Tukey's multiple-comparison test (n = 3). One-way ANOVA for each time point was instead done for data in C since two-way ANOVA requires matched data for all time points. Adjusted P values reflect *post hoc* comparisons between the responses of the WT cell line compared with the DKO cell line at the specific time point or DOX-treated cell line compared with a matched untreated cell line (n = 3). (C) Caspase 3/7 activities were measured using a luciferase assay from cells after 2 days of DOX treatment. Statistical differences were calculated using one-way ANOVA with Tukey's multiple-comparison test (n = 3). Error bars, standard error of mean. ns, not significant.

represent different stages of B cell maturation (Fig. 5A). It is possible that the stoichiometry of the BCL2 family members is a function of the stage of B cell differentiation.

If the skewed expression of MCL1 explains the dependency of PEL cell lines to this BCL2 family member, we expect that changing the ratios of the BCL2 family genes would shift the dependency to the most abundant BCL2 family protein and away from MCL1. We thus transduced BC-1 or BC-3 cells with lentiviruses constitutively expressing the different BCL2 genes under the major immediate early promoter and enhancer of the human cytomegalovirus at a multiplicity of infection (MOI) of 5. We chose to overexpress only the proteins that are expressed endogenously at the RNA and protein levels, as follows: BCL2, BCL-xL, BCL-W, or MCL1. In addition, we also expressed the KSHV homolog of BCL2, vBCL2 (35, 36), that has been dually tagged with FLAG-hemagglutinin (HA) epitopes at the N terminus (N-vBCL2). Although vBCL2 is a lytic gene and is not expressed in latently infected PEL cells, we were curious if it can functionally substitute for MCL1 in PEL. Western blots confirm that each protein is expressed above endogenous levels in both BC-1 and BC-3 backgrounds (Fig. 5B).

To confirm that the overexpressed proteins are functional in inhibiting intrinsic apoptosis, we induced cell death in these cell lines using staurosporine and measured cellular viability using CellTiterGlo 2.0 and apoptosis using the caspase 3/7 luciferase assay. All of the ectopically expressed BCL2 family proteins and vBCL2 reduced basal caspase 3/7 activity in the absence of staurosporine in both BC-1 and BC-3 cells (Fig. 5C and D). Reduction of caspase 3/7 activity was consistently stronger in the BC-1 cell lines than that in the BC-3 cell lines. In both cases, overexpression of BCL2, BCL-xL, or BCL-W inhibited basal caspase 3/7 activity the most, while MCL1 or N-vBCL2 had modest to no effects. It is possible that this minor effect of MCL1 or N-vBCL2 in decreasing basal caspase 3/7 activity may be due to insufficient overexpression of these proteins.

In the presence of staurosporine, naive and mCherry-expressing cells had significantly reduced cellular viability after overnight treatment as expected (Fig. 5E and F).

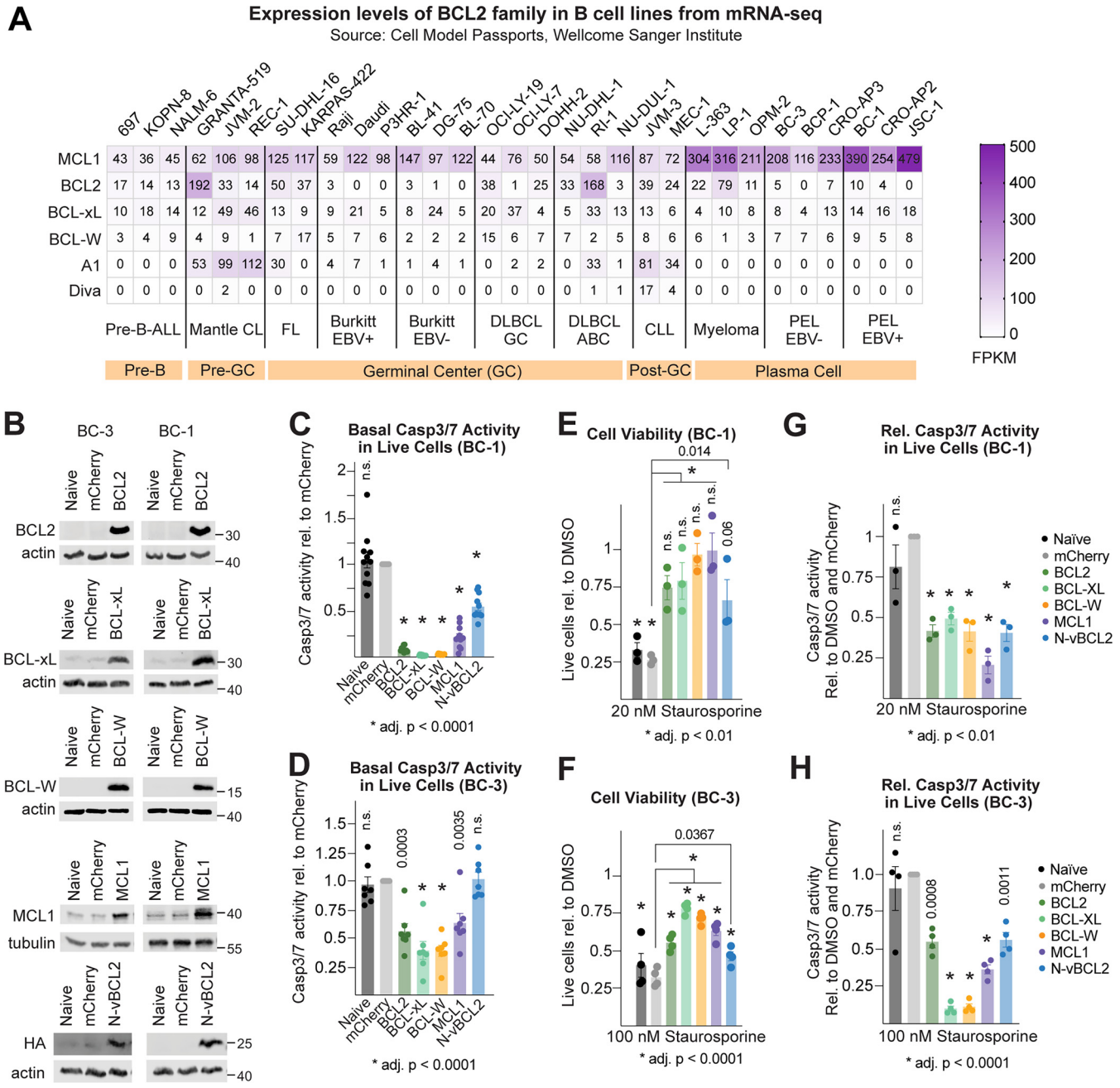

FIG 5 (A) Normalized expression values (fragments per kilobase of exon per million mapped fragments [FPKM]) of BCL2 family transcripts in B cell lines representing different malignancies and stage of B cell differentiation from the Cell Model Passports database (34). These cancers include pre-B cell acute lymphoblastic leukemia (pre-B-ALL), mantle cell lymphoma (mantle CL), follicular lymphoma (FL), Burkitt lymphoma (EBV-infected or uninfected), diffuse large B cell lymphoma germinal center subtype (DLBCL GC) or activated B cell subtype (DLBCL ABC), chronic lymphocytic leukemia (CLL), multiple myeloma, and PEL. (B) Western blots of the BCL2 family members and FLAG-HA-tagged vBCL2 in BC-1 or BC-3 cells transduced with lentiviruses overexpressing these cDNAs. (C and D) Basal caspase 3/7 activity of BC-1 (n = 11) or BC-3 cells (n = 7) normalized to total live cells measured by a caspase 3/7 luciferase assay. Cell viability measured by CellTiterGlo 2.0 assay (E and F) or relative caspase 3/7 activity in live BC-1 (n = 3) or BC-3 cells (n = 4) (G and H) after overnight treatment of 20 nM or 100 nM staurosporine. Statistical differences were calculated using one- or two-way ANOVA with Tukey's multiple comparison *post hoc* test. Adjusted *P* values reflect *post hoc* comparisons between the cell lines in response to staurosporine or DMSO unless indicated otherwise. Error bars, standard error of mean. n.s., not significant.

Cell death was rescued in all instances by all the BCL2 family proteins, including N-vBCL2, although to a lesser extent than the mCherry control. These effects on cell viability are conversely accompanied by a reduction in caspase 3/7 activities (Fig. 5G and H). These experiments demonstrate that the ectopically expressed BCL2 family proteins in BC-1 or BC-3 cells are functional in inhibiting intrinsic apoptosis.

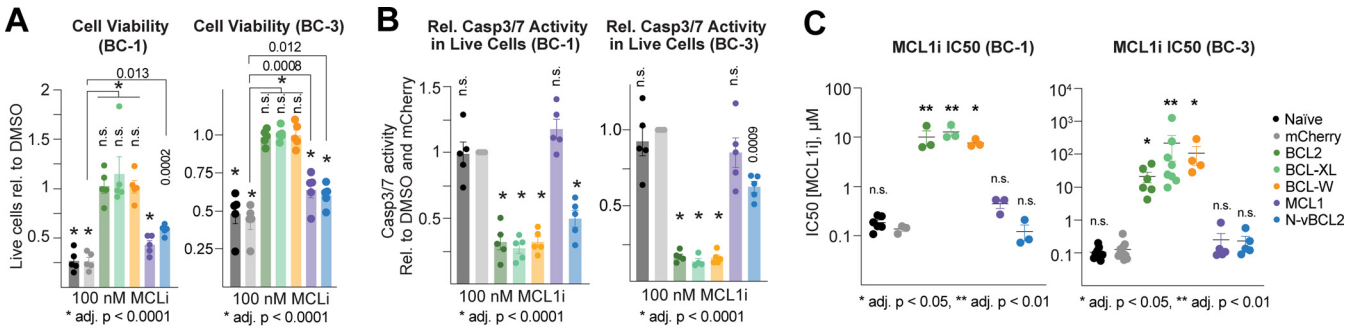

FIG 6 (A and B) Cell viability measured by CellTiterGlo 2.0 assay (B) or relative caspase 3/7 activity in live BC-1 or BC-3 cells overexpressing BCL2 family cDNAs (B) after overnight treatment of 100 nM MCL1i. Statistical differences were calculated using one- or two-way ANOVA with Tukey's multiple-comparison test ($n = 5$). Adjusted *P* values reflect *post hoc* comparisons between the cell lines in response to staurosporine or DMSO unless indicated otherwise. (C) IC_{50} values of MCL1i in BC-1 or BC-3 cells. For BC-1, one-way ANOVA with Tukey's multiple-comparison test was used for statistical tests ($n \geq 3$). Since BC-3 cell lines overexpressing BCL2, BCL-xL, or BCL-W were highly resistant to MCL1i even at high doses, IC_{50} values derived from these incomplete sigmoidal dose-response curves had low confidence intervals. Thus, nonparametric Kruskal-Wallis posttest was used. Adjusted *P* values reflect *post hoc* comparisons between the cell lines to the mCherry control. Error bars, standard error of mean. n.s., not significant.

Overexpression of BCL2 family proteins desensitizes PEL cells to MCL1i-induced apoptosis. We next tested whether overexpression of the BCL2-related proteins in BC-1 or BC-3 can shift the dependency to a different BCL2 family protein and cause cells to be less reliant on MCL1 for survival. We therefore inactivated MCL1 with MCL1i. Similar to staurosporine, overnight treatment with MCL1i reduced the viability of naive or mCherry-expressing cells (Fig. 6A). In contrast, ectopic BCL2, BCL-xL, or BCL-W fully protected BC-1 and BC-3 cells against MCL1i toxicity. N-vBCL2- and, surprisingly, MCL1-expressing cells were sensitive to MCL1i with only a marginal rescue of cell viability (20 to 30%) compared with mCherry. These effects in cell viability are likely due to apoptosis, as seen with the opposite pattern of caspase 3/7 activity in these cell lines (Fig. 6B). Relative to naive and mCherry-expressing cells, ectopic BCL2, BCL-xL, or BCL-W inhibited caspase 3/7 activity induced by MCL1i to the same degree in both BC-1 and BC-3. Ectopic N-vBCL2 moderately reduced caspase 3/7 activity, while MCL1 had no measurable effect.

Finally, we treated the cells with various doses of MCL1i to calculate their relative sensitivities to this inhibitor. Consistent with what we observed in Fig. 6A and B, overexpression of BCL2, BCL-xL or BCL-W desensitized cells from MCL1i and increased the IC_{50} values by 100- to 1,000-fold (Fig. 6C). The N-vBCL2 construct did not alter the overall sensitivities of BC-1 or BC-3 cells to MCL1i. While ectopic MCL1 increased the average MCL1i IC_{50} by ~2- (BC-3) to 3-fold (BC-1), these effects were not statistically significant. In summary, our data demonstrate that expression levels of the BCL2 family genes are the major determinant for the dependency on MCL1 by PEL cell lines.

DISCUSSION

In this report, we explore why KSHV-transformed PEL cell lines exhibit selective addiction to the oncogene MCL1, despite having shared functions with the related BCL2 family proteins. While new roles beyond those shared with the other BCL2 family members have been attributed to MCL1, we show that the essential function of MCL1 in PEL cell lines is to prevent intrinsic apoptosis. This selective addiction to MCL1 is explained by the 15- to 60-fold stoichiometric excess of MCL1 expression relative to other BCL2-related proteins, as demonstrated by mRNA-seq and functional rescue from MCL1i-induced cell death by overexpression of any of the BCL2 family proteins.

The failure to rescue MCL1i-induced apoptosis by the MCL1 or N-vBCL2 constructs may be due to the degree of ectopic expression achieved in these cells. It is possible that the total amount of BCL2 family proteins in any of these cases did not reach the minimum required to neutralize all available MCL1i molecules.

It is not clear why BCL2 family expression is skewed toward MCL1 in PEL cell lines. We speculate that it may be a consequence of the plasma cell-like B cell differentiation

stage of PEL tumors (4–6). Similarly, Fig. 5A and the Cancer Dependency Map (37) show that multiple myeloma cell lines, which are considered to be of plasma cell lineage, have high MCL1 expression and are selectively dependent on MCL1. In contrast, cell lines derived from B cell malignancies representing earlier B cell stages have distinct expression patterns where the other BCL2 family members are expressed at higher levels (Fig. 5A). Studies done in mice by the Tarlinton group indicate that the requirements for the Bcl2 family members during B cell development are dynamic and complex. It was shown that Mcl1 but not Bcl-xL is required for the formation but not persistence of germinal center B cells and memory B cells using conditional knockout models (38). These data point to a transient dependence of antigen-specific B cells on Mcl1 for competition within germinal centers during maturation but not for their survival after their establishment. Mcl1, however, is indispensable for the survival of plasma cells in culture and *in vivo* in a tamoxifen-inducible Mcl1 knockout mouse model in a cell intrinsic manner (39). In contrast, inducible knockout of Bcl-xL or treatment with ABT-737, a preferential inhibitor of BCL2 with modest effects on Bcl-xL and Bcl-W, has no effect on the survival of existing plasma cells in culture or *in vivo*, respectively (39, 40). They propose that plasma cells require high levels of Mcl1 along with other factors to provide an intrinsic survival potential in combination with extrinsic survival signals from tissue-specific niches (e.g., secondary lymphoid tissues or bone marrow) to ensure long-lived plasma cells (41). The requirement for the high expression of MCL1 in plasma cells may be driven by master transcription factors, such as IRF4, that occupy lineage-specific superenhancer regulatory regions. Indeed, we and others have identified a superenhancer element around the MCL1 locus bound by IRF4 in PEL cell lines (21, 42, 43).

Upon activation and during maturation, B cells undergo dramatic changes to support their effector functions in immune defense (reviewed in reference 44). A large part of the plasma cell differentiation program is the remodeling and expansion of the endoplasmic reticulum (ER) to prepare for immunoglobulin production and secretion (45). Nutrient transporters and metabolic enzymes are upregulated to sustain antibody production and organelle maintenance by the lineage transcription factor Blimp-1 (46). High expression of MCL1 may thus act as a buffer from this increased ER stress and metabolic load to ensure the survival of these B cells. Knockdown of the glucose transporter GLUT4 in multiple myeloma cell lines induced apoptosis by decreasing MCL1 mRNA expression (47), thereby supporting this link between metabolism and apoptosis.

In the case of PEL, the infected tumor cells neither express nor secrete immunoglobulin molecules. However, recent work from the Gottwein laboratory shows that PEL cell lines need to constitutively counteract death signals originating from the ER and Golgi compartments in the absence of any exogenous trigger (48). Consistent with this finding, PEL cell lines have an elevated expression of genes involved in the unfolded protein response, which are often triggered by ER stress (4). These results suggest that the ER and Golgi bodies in PEL cells are also under stress despite the absence of antibody production. In line with this idea, KSHV is known to activate ER stress responses during lytic reactivation (49, 50). Therefore, KSHV needs to counter these ER, Golgi, and metabolic stresses by possibly reinforcing or amplifying existing survival pathways in plasma cells, such as MCL1. More recently, the latency-associated nuclear antigen (LANA) was shown to indirectly enhance the steady-state levels of the MCL1 protein by binding to the E3 ubiquitin ligase FBW7 and preventing MCL1 degradation (51). As mentioned above, although we find binding sites for the lineage transcription factor IRF4 on the MCL1 superenhancer in PEL cells, we reported recently that the B cell-specific latency gene vIRF3 largely co-occupies similar sites as IRF4, including the MCL1 superenhancer and promoter (21). This finding suggests that vIRF3 may function to enhance MCL1 expression. We are currently investigating how vIRF3 regulates MCL1 expression at the transcriptional level.

A parallel relationship between lineage-specific expression and dependence to the BCL2 family proteins is also seen in lymphatic endothelial cells (LECs) which are thought to be candidates for the cellular origin of Kaposi's sarcoma spindle cells (52). In this case, LECs

express and depend on high levels of BCL-xL instead of MCL1 for survival. This dependency dramatically increases during KSHV infection (Michael Lagunoff, personal communication) which supports the model where the virus reinforces prosurvival pathways already present in the cell.

The selective dependence of PEL cell lines to MCL1 makes it an attractive target for therapy. We have shown previously that the MCL1 protein is highly expressed in primary tumors from patients (26). Candidate MCL1-selective drugs are now in various stages of clinical trials to treat hematologic malignancies (53) and have the potential to be repurposed to treat PEL. Venetoclax, the first approved BH3 mimetic drug, has overall response rates of ~80% in relapsed and/or refractory chronic lymphocytic leukemia (54) and ~75% in relapsed and/or refractory mantle cell lymphoma (55) with a durable response even after ~3 years (56). However, other cancers like acute myelogenous leukemia exhibit a lower response rate to venetoclax (19%) where nonresponsive patients had an increase in BCL-xL or MCL1 expression (57). Our data similarly show that overexpression of any of the BCL2 family proteins or a loss of BAX or BAK1 leads to resistance to MCL1 inhibitors. Thus, care must be taken when testing MCL1 inhibitors in PEL patients to avoid resistance. One strategy is using high but tolerable doses of MCL1 drugs to minimize selection for resistant tumor cells. Another approach is to combine this treatment with other regimens that do not act on the same pathway. These strategies need to be explored to provide the most effective treatment for KSHV-induced PEL.

MATERIALS AND METHODS

Cells. Cells were cultured as described (21). HEK293T cells were cultured in Dulbecco's modified Eagle medium with L-glutamine and 4.5 g/L glucose (Corning Life Sciences, Tewksbury, MA) supplemented with 10% Serum Plus II medium (Millipore-Sigma, Burlington, MA) and 10 μg/mL gentamicin (Gibco, Waltham, MA). BC-1 and BC-3 cell lines were grown in RPMI 1640 (Corning) supplemented with 10 μg/mL gentamicin (Life Technologies, Carlsbad, CA), 0.05 mM β-mercaptoethanol (Sigma-Aldrich, St. Louis, MO), and 10% (BC-1) or 20% (BC-3) Serum Plus II medium. All PEL cell lines were grown at 37°C with 5% CO_2 and maintained at log phase between 2×10^5 and 1×10^6 cells/mL.

Primers and synthetic genes. All primers were purchased from Integrated DNA Technologies (Coralville, IO). Synthetic genes for the enhanced green fluorescent protein (eGFP) fragment, shRNA cassettes, and MCL1 cDNA were synthesized by Twist Bioscience (South San Francisco, CA). Sequences and primer combinations for cloning are listed in Table 1 and 2.

shRNAs. A self-inactivating version of the pLVX-TetOne-Zeo lentiviral vector (58) (a gift from Britt Glaunsinger) was first made via PCR mutagenesis. A deletion in the U3 region of the 3′ long terminal repeat (LTR) was introduced using primer pairs 169/171 and 172/170. The PCR products were fused with primers 169/170 and cloned into pLVX-TetOne-Zeo using the KpnI and NheI restriction sites (New England BioLabs [NEB], Ipswich, MA). The new vector is renamed pLVX-SIN-TetOne-Zeo (pSTZ) to denote the self-inactivating deletion (SIN).

shRNAs were designed using the SplashRNA algorithm (33) using default parameters (http://splashrna.mskcc.org). sh2MCL1 was synthesized as a gene fragment (Twist Bioscience), while shREN was amplified from pZIP-ZsGreen-T2A-Hyg-shRen.713 (48). These shRNA cassettes were assembled in the 3′ untranslated region (UTR) of a synthetic eGFP gene (Twist Bioscience) via two-fragment Gibson assembly into the pSTZ backbone linearized by EcoRI and BamHI (NEB).

BCL2 cDNAs. cDNAs for human BCL2, BCL-xL, and BCL-W were amplified from pCDNA3-HA-BCL2, pCDNA-HA-BCL-xL (59) (gifts from Timothy Chambers), and pLX304-BCL2L2 (clone HsCD00440394 from Human ORFeome Collection from DNASU [60]). The vBCL2 sequence was amplified from BC-1 genomic DNA. The Flag-HA dual tag cassette was amplified from pLC-FLAG-HA-vIRF3-P2A-hyg (M. Manzano and E. Gottwein, unpublished). Internal restriction sites were repaired using PCR mutagenesis. Details on primer sequences and primer combinations for each PCR step are listed in Table 1 and 2.

Lentiviruses. The day prior to transfections, 4×10^6 to 5×10^6 293T cells were plated in 10-cm dishes. Lentiviral transfer vectors (5 μg) were cotransfected with pMD2.G (2.44 μg) and psPAX2 (3.74 μg) packaging vectors and 39.13 μL 1 mg/mL polyethylenimine (catalog no. 408727; Sigma) in 500 μL Opti-MEM (Gibco). After 4 to 6 h, medium was replaced with complete RPMI medium supplemented with 10% Serum Plus II medium. Supernatants containing lentiviruses were harvested after 3 days by filtering through a 0.45-μm-pore membrane.

Lentiviral titers were determined by functional titration. Increasing volumes of supernatant containing lentiviruses were added to 1×10^5 naive BC-1 or BC-3 cells in 0.5 mL media with 0.5 μL 8 μg/mL Polybrene. The day after, appropriate antibiotics were added to select for infected cells. The number of surviving cells was compared to uninfected cells to determine infection rates and viral titers. Final lentiviral transductions were performed in 4×10^5 BC-1 or BC-3 cells in 2 mL media with 8 μg/mL Polybrene at defined MOIs.

Generation of BAX/BAK1 DKO cells. Two gRNAs targeting the human *BAX* or *BAK1* gene were chosen from the genome-wide Brunello CRISPR library to increase the efficiency of editing in all alleles (61).

TABLE 1 Primer sequences

Primer name	Sequence
5	CACCGACGGCAGCTCGCCATCATCG
6	AAACCGATGATGGCGAGCTGCCGTC
50	GCTAGCGCTACCGGTGCCGCCACCATGGCGCACGCTGGGAGAACAGGG
51	GGGAGAGGGGCGGATCCTCACTTGTGGCCCAGATAGGC
54	GCTAGCGCTACCGGTGCCGCCACCATGTCTCAGAGCAACCGGGAGCTGG
55	GGGAGAGGGGCGGATCCTCATTTCCGACTGAAGAGTGAGCCC
56	CCACCTAGAGCCTTGGATTCAGGAGAACGGCGGCTGG
57	CCAGCCGCCGTTCTCCTGAATCCAAGGCTCTAGGTGG
62	GCTAGCGCTACCGGTGCCGCCACCATGGCGACCCCAGCCTCGGCCCCAG
63	GGGAGAGGGGCGGATCCTCACTTGCTAGCAAAAAAGGCCCCTAC
64	GCAGCTGGCTGACTGGATTCACAGCAGTGGGGGCTGG
65	CCAGCCCCCACTGCTGTGAATCCAGTCAGCCAGCTGC
66	CCCGATTACGCTAGCGGCGACGAGGACGTTTTGCCT
67	AGGCAAAACGTCCTCGTCGCCGCTAGCGTAATCGGG
68	GAGATTTCACAGCACCACTGGTATAAACCAGCTTGGG
69	CCCAAGCTGGTTTATACCAGTGGTGCTGTGAAATCTC
70	GGGAGAGGGGCGGATCCTTATCTCCTGCTCATCGCGACCGC
97	CACCGTTTCATCCAGGATCGAGCA
98	AAACTGCTCGATCCTGGATGAAAC
99	CACCGGACGAACTGGACAGTAACA
100	AAACTGTTACTGTCCAGTTCGTCC
103F	CACCGCTCACCTGCTAGGTTGCAG
103R	AAACCTGCAACCTAGCAGGTGAGC
161	GACACCGGTGCAGCGGCCGCTGTTTGAATGAGGCTTCAGTAC
162	GTCCAGCTTAGCTCGCAGGGGAGGTGGTCTGGATCCTAAAGTGATTTAATTTATACCATT
169	CTACCAATGCTGATTGTGCCTGGC
170	AACAGCTATGACCATGATTACGCC
171	CTAACCAGAGAGACCCAGTACAGTCCGGATGCAGCTCTCGGGCCAC
172	GTGGCCCGAGAGCTGCATCCGGACTGTACTGGGTCTCTCTGGTTAG
189	GAGTTTGAGGTCTGATTATTGTGG
190	GAAGTTGCCGTCAGAAAACATGTC
197	CACCGGCCTTCTTTGAGTTCGGTG
198	AAACCACCGAACTCAAAGAAGGCC
199	CACCGCTGACGCCCTTCACCGCGCG
200	AAACCGCGCGGTGAAGGGCGTCAGC
215	CTCCCTGACTCCCAGCTTTG
216	CCTGGTGGCAATCTTGGTGA
219	CACCGAGACAAAGAAGGCTACAAGG
220	AAACCCTTGTAGCCTTCTTTGTCTC
221	CACCGTGTGCTGAGAGTGTCAACA
222	AAACTGTTGACACTCTCAGCACAC
EHG4087	GAGCTGGTTTAGTGAACCG
eGFP cassette	ACTTTCCGTACCACTTCCTACCCTCGTAAAGAATTCATGGTGAGCAAGGGCGAGGAGCTGTTCACCGGGGTGGTGCCCATCCTGGT CGAGCTGGACGGCGACGTAAACGGCCACAAGTTCAGCGTGTCCGGCGAGGGCGAGGGCGATGCCACCTACGGCAAGCTGACCC TGAAGTTCATCTGCACCACCGGCAAGCTGCCCGTGCCCTGGCCCACCCTCGTGACCACCCTGACCTACGGCGTGCAGTGCTTCAGCC GCTACCCCGACCACATGAAGCAGCACGACTTCTTCAAGTCCGCCATGCCCGAAGGCTACGTCCAGGAGCGCACCATCTTCTTCAA GGACGACGGCAACTACAAGACCCGCGCCGAGGTGAAGTTCGAGGGCGACACCCTGGTGAACCGCATCGAGCT GAAGGGCATCGACTTCAAGGAGGACGGCAACATCCTGGGGCACAAGCTGGAGTACAACTACAACAGCCACAACGTCTAT ATCATGGCCGACAAGCAGAAGAACGGCATCAAGGTGAACTTCAAGATCCGCCACAACATCGAGGACGGCAGCGTGCAG CTCGCCGACCACTACCAGCAGAACACCCCCATCGGCGACGGCCCCGTGCTGCTGCCCGACAACCACTACCTGAGCACCC AGTCCGCCCTGAGCAAAGACCCCAACGAGAAGCGCGATCACATGGTCCTGCTGGAGTTCGTGACCGCCGCCGGGATCAC TCTCGGCATGGACGAGCTGTACAAGTAGGACACCGGTGCAGCGGCCGCTGTTTGAATGAGGCTTCAGTACTTTACAGA
sh2MCL1 cassette	TGTTTGAATGAGGCTTCAGTACTTTACAGAATCGTTGCCTGCACATCTTGGAAACACTTGCTGGGATTACTTCTTCAGGTTA ACCCAACAGAAGGCTAAAGAAGGTATATTGCTGTTGACAGTGAGCGCTCCCAGTATACTTCTTAGAAATAGTGAAGCCACA GATGTATTTCTAAGAAGTATACTGGGAATGCCTACTGCCTCGGACTTCAAGGGGCTACTTTAGGAGCAATTATCTTG TTTACTAAAACTGAATACCTTGCTATCTCTTTGATACATTTTTACAAAGCTGAATTAAAATGGTATAAATTAAATC ACTTTAGGATCCAGACCACCTCCCCTGCGAGCTAAGCTGGAC

Based on these gRNAs, primer pairs were designed to create double-stranded DNA (dsDNA) duplexes with compatible BbsI overhangs. These primer pairs were assembled by heat-denaturation and annealing in Buffer 3.1 (NEB) and then cloned into BbsI-linearized pX458 (62) (a gift from Feng Zhang; Addgene no. 48138).

TABLE 2 Combinations of primers used for cloning constructs

Construct	PCR run	Primer name	Template	Source
pLV-SIN-TetOne-ZeoR (pSTZ)	1	169, 171	pLVX-TetOne-Zeo	58
	2	170, 172		
	Overlap	169, 170	PCR 1 and 2	
shREN	N/A	161, 162	pZIP-ZsGreen-T2A-Hyg-shRen.713	48
BCL2	N/A	50, 51	pCDNA3 HA-BCL2	59
BCL-xL	1	54, 57	pcDNA3 HA-BCL-xL	
	2	55, 56		
	Overlap	54, 55	PCR 1 and 2	
BCL-W	1	62, 65	pLX304 BCL2L2	DNASU
	2	63, 64		
	Overlap	62, 63	PCR 1 and 2	
vBCL2 N-FLAG-HA	1	EHG4087, 67	pLC-FLAG-HA-vIRF3-P2A-hyg	M. Manzano and E. Gottwein, unpublished
	2	66, 69	BC-1 genomic DNA	
	3	68, 70	BC-1 genomic DNA	
	1 + 2	EHG4087, 69	PCR 1 and 2	
	Final	EHG4087, 70	PCR 1 + 2 and 3	
BAX g2	Anneal	97, 98		
BAX g3	Anneal	99, 100		
BAK1 g1	Anneal	5, 6		
BAK1 g2	Anneal	103F, 103R		
BCL2 g1	Anneal	197, 198		
BCL2 g2	Anneal	199, 200		
BCL-W g1	Anneal	219, 220		
BCL-W g2	Anneal	221, 222		

BC-3 cells were adjusted to 2×10^5 cells/mL the day before transfection. On the day of transfection, 1×10^6 BC-1 or BC-3 cells were pelleted in 50-mL tubes at 90 $\times$ *g*, for 10 min. Each pellet was carefully resuspended in 20 μL of SF cell line nucleofector solution with supplement 1 (catalog no. V4XC-2032; Lonza, Basel, Switzerland) and 1.5 μL of pX458 plasmids (150 ng each of BAX g2, BAX g3, BAK1 g1, and BAK1 g3; 600 ng total). Cells transferred to Nucleocuvette strips and pulsed with program CA-189 using the 4D-Nucleofector X system (Lonza). Transfection reactions were allowed to recover at room temperature for 10 min. Afterward, 80 μL of prewarmed complete medium was added. Cells in the Nucleocuvette strips were incubated at 37°C for 10 min. Finally, cells were collected with an additional 120 μL of prewarmed complete media and transferred to a round-bottom 96-well plate. Cells were expanded for 5 to 7 days to at least 2×10^6 total cells. Two additional rounds of nucleofection were performed as described above to ensure efficient editing in all four alleles.

After a week of recovery from the third nucleofection, cells were cultured individually in a round-bottom 96-well plate using dilution cloning. Clones were screened for successful editing. We first triaged the clones based on the absence of full-length BAX and BAK1 proteins by Western blotting. Next, we further screened clones using genotyping primers (189 and 190 for *BAX*; 215 and 216 for *BAK1*). We would expect that simultaneous cutting of the two guides in an allele will lead to ~100- to 400-bp deletions that can be distinguished from WT or single-cut alleles by PCR. While this assay does not discriminate between unedited from single editing events, it allows us to limit our final validation to those with at least one allele deleted. Finally, we confirmed frameshift indels by amplifying the targeted loci for Sanger or Illumina sequencing. Illumina sequencing and analysis were performed by the Massachusetts General Hospital Center for Computational and Integrative Biology DNA Core Facility.

CRISPR targeting of BCL2 family. Clonal BC-1 Cas9 or BC-3 Cas9 cells (26) were transduced with lentiviruses encoding gRNAs targeting the BCL2 family genes at an MOI of 1. gRNAs targeting BCL2 or BCL-W were cloned in pLentiGuide (Addgene no. 117986) that was linearized with BsmBI (NEB). gRNAs for gAAVS1, BCL-xL, and MCL1 have been cloned and described previously (26). Live cells were measured every 2 to 3 days on the fluorescence-activated cell sorter (FACS) Celesta flow cytometer (BD Biosciences, Franklin Lakes, NJ) using a known amount of spike-in AccuCount Blank particles (catalog no. ACBP-50-10; Spherotech, Lake Forest, IL). Data analysis was performed using FlowJo v10.8.1 software (BD Biosciences). Cells were split to 3×10^5 cells/mL to ensure that all cells were dividing continuously.

Western blots. Cells were washed with phosphate-buffered saline and lysed with radioimmunoprecipitation assay (RIPA) lysis buffer (50 mM Tris, 150 mM NaCl, 1% IGEPAL CA-630, 0.5% sodium deoxycholate, and 0.1% sodium dodecyl sulfate [pH 7.4]) with protease inhibitor cocktail III (Calbiochem, EMD Millipore). Lysates were incubated on ice for 10 min and clarified by spinning at 12,000 $\times$ *g* for 10 min. Total protein was quantified with the Pierce BCA protein assay kit (Thermo Fisher).

Equivalent amounts of total proteins were run in Bolt 4% to 12% Bis-Tris gradient gels (Thermo Fisher Scientific) or 15% tris-glycine-SDS acrylamide gels and transferred to 0.2-μm-pore size nitrocellulose membranes in Towbin buffer (25 mM Tris, 192 mM glycine, and 20% methanol [pH 8.3]) for 90 min at 400 mA. Membranes were blocked with a 1:3 dilution of intercept (TBS) protein-free blocking buffer (Li-Cor Biosciences, Lincoln, NE) in TBS for 1 h at room temperature. Membranes were incubated with

primary antibodies diluted 1:3,000 in blocking buffer plus 0.1% Tween 20 overnight at 4°C. Primary antibodies were purchased from Cell Signaling Technology (Danvers, MA), namely, anti-BCL2 clone D55G8, anti-BCL-xL clone 54H6, anti-BCL-W clone 31H4, anti-MCL1 clone D2W9E, anti-HA clone C29F4, anti-A1 clone D1A1C, anti-Diva (catalog no. 3869), anti-BAK clone D4E4, and anti-BAX clone D2E11; from Sigma, namely, anti-beta-actin clone AC-15 and anti-alpha-tubulin clone B-5-1-2; or Santa Cruz Biotechnology (Dallas, TX), namely, anti-GAPDH clone 0411.

Immunoblots were washed five times with TBS with Tween (TBST) for 5 min each and then incubated for 1 h with IRDye 800 CW-conjugated secondary antibodies (Li-Cor Biosciences) diluted in TBS (1:20,000). Membranes were finally washed four times with TBST and once in TBS. Western blots were imaged on the Odyssey Fc or M Imager system (Li-Cor Biosciences).

Dose-response curves. Serial dilutions of the different inhibitors/drugs were added to each well containing 5×10^3 BC-1 or BC-3 cells in a U-bottom 96-well plate. At designated time points (2 days for puromycin [Cayman Chemicals, Ann Arbor, MI]; 3 days for MCL1i [MedChemExpress, Monmouth Junction, NJ], ABT-199 [Tocris Bioscience, Minneapolis, MN], WEHI-539 [APExBIO, Houston, TX], and staurosporine [APExBIO]; and 6 days for blasticidin [Gibco], zeocin [Invivogen, San Diego, CA], and hygromycin [Gibco]), 20-μL aliquots of the cells were used to measure cell viability using 20 μL CellTiter-Glo 2.0 cell viability reagent (Promega). Luminescence was read using a Synergy H1 microplate reader (Biotek, Winooski, VT) with an integration time of 2 sec. Raw luminescence readings were normalized as a percentage of the DMSO control. Normalized values were used to calculate the IC_{50} using the "[inhibitor] versus normalized response (variable slope)" function in Prism 9 (GraphPad, San Diego, CA).

Caspase 3/7 assay. A total of 2×10^4 BC-1 or BC-3 cells were seeded in each well of a U-bottom 96-well plate and treated with staurosporine (20 nM for BC-1 or 100 nM for BC-3), 100 nM MCL1i, or DMSO. These concentrations were chosen because they approximate the IC_{50} values of each drug for each cell line. After 24 h, 20 μL of cells was mixed with 20 μL of the CellTiter-Glo 2.0 cell viability reagent or Caspase-Glo 3/7 assay substrate (Promega). Luminescence was measured after a 2-min incubation for CellTiter-Glo 2.0 or a 30-min incubation for the Caspase-Glo 3/7 assay using the Synergy H1 microplate reader as described above. Raw luminescence values for caspase 3/7 activities were sequentially normalized to the matched raw CellTiter-Glo 2.0 readings, then to the DMSO controls, and finally to the mCherry-expressing cell line.

Annexin V/7-AAD staining. BC-1 or BC-3 WT or DKO cells (4×10^5 cells/mL, 3 mL plated in a 6-well plate) were treated overnight with DMSO, 20 nM staurosporine, or 100 nM MCL1i. A total of 7×10^5 live cells were pelleted and washed twice with wash buffer (2% bovine serum albumin in phosphate-buffered saline [PBS]). Cells were resuspended in 100 μL annexin V binding buffer (Biolegend, San Diego, CA). Cells were stained for 15 min in the dark with 5 μL APC annexin V (Biolegend) and 5 μL 7-AAD viability staining solution (Biolegend). After incubation, 400 μL of annexin V binding buffer was added and the cells were analyzed on a flow cytometer. In parallel, cellular viability and caspase 3/7 activities were measured as described above from 20-μL aliquots.

ACKNOWLEDGMENTS

We thank Logan Moorhead for initial help with engineering the DKO cell lines, Eva Gottwein for the pZIP-ZsGreen-T2A-Hyg-shRen.713 and pLC-FLAG-HA-vIRF3-P2A-hyg plasmids, Britt Glaunsinger for the pLVX-TetOneZeo plasmid, and Timothy Chambers for the BCL-xL and BCL2 expression vectors. We thank Eva Gottwein, Youssef Aachoui, Changhoon Oh, and J. Craig Forrest for helpful discussion and feedback on the manuscript.

This work is supported by a Transition Career Development Award (K22 CA241355) from the National Cancer Institute of the National Institutes of Health (NIH) to M.M. Additional support was provided by the Center for Microbial Pathogenesis and Host Inflammatory Responses program grant P20 GM103625 from the National Institute of General Medical Sciences (NIGMS) of the NIH, Winthrop P. Rockefeller Cancer Institute at UAMS, and an equipment grant from the UAMS Office of the Vice Chancellor for Research and Innovation. J.G. is a recipient of the Undergraduate Summer Research Fellowship from the Arkansas IDeA Network of Biomedical Research Excellence (INBRE) funded by program grant P20 GM103429 from NIH/NIGMS. The content is solely the responsibility of the authors and does not necessarily represent the official views of the funding bodies.

We declare no conflicts of interests.

REFERENCES

1. Cesarman E. 2014. Gammaherpesviruses and lymphoproliferative disorders. Annu Rev Pathol 9:349–372. https://doi.org/10.1146/annurev-pathol-012513-104656.
2. Nador RG, Cesarman E, Chadburn A, Dawson DB, Ansari MQ, Sald J, Knowles DM. 1996. Primary effusion lymphoma: a distinct clinicopathologic entity associated with the Kaposi's sarcoma-associated herpes virus. Blood 88:645–656. https://doi.org/10.1182/blood.V88.2.645.bloodjournal882645.
3. Lurain K, Polizzotto MN, Aleman K, Bhutani M, Wyvill KM, Goncalves PH, Ramaswami R, Marshall VA, Miley W, Steinberg SM, Little RF, Wilson W, Filie AC, Pittaluga S, Jaffe ES, Whitby D, Yarchoan R, Uldrick TS. 2019. Viral, immunologic, and clinical features of primary effusion lymphoma. Blood 133:1753–1761. https://doi.org/10.1182/blood-2019-01-893339.
4. Jenner RG, Maillard K, Cattini N, Weiss RA, Boshoff C, Wooster R, Kellam P. 2003. Kaposi's sarcoma-associated herpesvirus-infected primary effusion

lymphoma has a plasma cell gene expression profile. Proc Natl Acad Sci U S A 100:10399–10404. https://doi.org/10.1073/pnas.1630810100.
5. Klein U, Gloghini A, Gaidano G, Chadburn A, Cesarman E, Dalla-Favera R, Carbone A. 2003. Gene expression profile analysis of AIDS-related primary effusion lymphoma (PEL) suggests a plasmablastic derivation and identifies PEL-specific transcripts. Blood 101:4115–4121. https://doi.org/10.1182/blood-2002-10-3090.
6. Fan W, Bubman D, Chadburn A, Harrington WJ, Jr, Cesarman E, Knowles DM. 2005. Distinct subsets of primary effusion lymphoma can be identified based on their cellular gene expression profile and viral association. J Virol 79:1244–1251. https://doi.org/10.1128/JVI.79.2.1244-1251.2005.
7. Carbone A, Gloghini A, Cozzi MR, Capello D, Steffan A, Monini P, De Marco L, Gaidano G. 2000. Expression of MUM1/IRF4 selectively clusters with primary effusion lymphoma among lymphomatous effusions: implications for disease histogenesis and pathogenesis. Br J Haematol 111:247–257. https://doi.org/10.1046/j.1365-2141.2000.02329.x.
8. Petre CE, Sin SH, Dittmer DP. 2007. Functional p53 signaling in Kaposi's sarcoma-associated herpesvirus lymphomas: implications for therapy. J Virol 81:1912–1922. https://doi.org/10.1128/JVI.01757-06.
9. Bubman D, Guasparri I, Cesarman E. 2007. Deregulation of c-Myc in primary effusion lymphoma by Kaposi's sarcoma herpesvirus latency-associated nuclear antigen. Oncogene 26:4979–4986. https://doi.org/10.1038/sj.onc.1210299.
10. Gaidano G, Capello D, Cilia AM, Gloghini A, Perin T, Quattrone S, Migliazza A, Lo Coco F, Saglio G, Ascoli V, Carbone A. 1999. Genetic characterization of HHV-8/KSHV-positive primary effusion lymphoma reveals frequent mutations of BCL6: implications for disease pathogenesis and histogenesis. Genes Chromosom Cancer 24:16–23. https://doi.org/10.1002/(SICI)1098-2264(199901)24:1<16::AID-GCC3>3.0.CO;2-F.
11. Roy D, Sin SH, Damania B, Dittmer DP. 2011. Tumor suppressor genes FHIT and WWOX are deleted in primary effusion lymphoma (PEL) cell lines. Blood 118:e32–e39. https://doi.org/10.1182/blood-2010-12-323659.
12. Godfrey A, Anderson J, Papanastasiou A, Takeuchi Y, Boshoff C. 2005. Inhibiting primary effusion lymphoma by lentiviral vectors encoding short hairpin RNA. Blood 105:2510–2518. https://doi.org/10.1182/blood-2004-08-3052.
13. Wies E, Mori Y, Hahn A, Kremmer E, Sturzl M, Fleckenstein B, Neipel F. 2008. The viral interferon-regulatory factor-3 is required for the survival of KSHV-infected primary effusion lymphoma cells. Blood 111:320–327. https://doi.org/10.1182/blood-2007-05-092288.
14. Xiang Q, Ju H, Nicholas J. 2020. USP7-dependent regulation of TRAF activation and signaling by a viral interferon regulatory factor homologue. J Virol 94:e01553-19. https://doi.org/10.1128/JVI.01553-19.
15. Xiang Q, Ju H, Li Q, Mei SC, Chen D, Choi YB, Nicholas J. 2018. Human herpesvirus 8 interferon regulatory factors 1 and 3 mediate replication and latency activities via interactions with USP7 deubiquitinase. J Virol 92:e02003-17. https://doi.org/10.1128/JVI.02003-17.
16. Chen D, Sandford G, Nicholas J. 2009. Intracellular signaling mechanisms and activities of human herpesvirus 8 interleukin-6. J Virol 83:722–733. https://doi.org/10.1128/JVI.01517-08.
17. Bhatt AP, Bhende PM, Sin SH, Roy D, Dittmer DP, Damania B. 2010. Dual inhibition of PI3K and mTOR inhibits autocrine and paracrine proliferative loops in PI3K/Akt/mTOR-addicted lymphomas. Blood 115:4455–4463. https://doi.org/10.1182/blood-2009-10-251082.
18. Cousins E, Nicholas J. 2013. Role of human herpesvirus 8 interleukin-6-activated gp130 signal transducer in primary effusion lymphoma cell growth and viability. J Virol 87:10816–10827. https://doi.org/10.1128/JVI.02047-13.
19. de Oliveira DE, Ballon G, Cesarman E. 2010. NF-kappaB signaling modulation by EBV and KSHV. Trends Microbiol 18:248–257. https://doi.org/10.1016/j.tim.2010.04.001.
20. Gopalakrishnan R, Matta H, Tolani B, Triche T, Jr, Chaudhary PM. 2016. Immunomodulatory drugs target IKZF1-IRF4-MYC axis in primary effusion lymphoma in a cereblon-dependent manner and display synergistic cytotoxicity with BRD4 inhibitors. Oncogene 35:1797–1810. https://doi.org/10.1038/onc.2015.245.
21. Manzano M, Gunther T, Ju H, Nicholas J, Bartom ET, Grundhoff A, Gottwein E. 2020. Kaposi's sarcoma-associated herpesvirus drives a super-enhancer-mediated survival gene expression program in primary effusion lymphoma. mBio 11:e01457-20. https://doi.org/10.1128/mBio.01457-20.
22. Patil A, Manzano M, Gottwein E. 2018. CK1alpha and IRF4 are essential and independent effectors of immunomodulatory drugs in primary effusion lymphoma. Blood 132:577–586. https://doi.org/10.1182/blood-2018-01-828418.
23. Sarek G, Kurki S, Enback J, Iotzova G, Haas J, Laakkonen P, Laiho M, Ojala PM. 2007. Reactivation of the p53 pathway as a treatment modality for KSHV-induced lymphomas. J Clin Invest 117:1019–1028. https://doi.org/10.1172/JCI30945.
24. Sin SH, Roy D, Wang L, Staudt MR, Fakhari FD, Patel DD, Henry D, Harrington WJ, Jr, Damania BA, Dittmer DP. 2007. Rapamycin is efficacious against primary effusion lymphoma (PEL) cell lines in vivo by inhibiting autocrine signaling. Blood 109:2165–2173. https://doi.org/10.1182/blood-2006-06-028092.
25. Keller SA, Schattner EJ, Cesarman E. 2000. Inhibition of NF-kappa B induces apoptosis of KSHV-infected primary effusion lymphoma cells. Blood 96:2537–2542. https://doi.org/10.1182/blood.V96.7.2537.
26. Manzano M, Patil A, Waldrop A, Dave SS, Behdad A, Gottwein E. 2018. Gene essentiality landscape and druggable oncogenic dependencies in herpesviral primary effusion lymphoma. Nat Commun 9:3263. https://doi.org/10.1038/s41467-018-05506-9.
27. Westphal D, Kluck RM, Dewson G. 2014. Building blocks of the apoptotic pore: how Bax and Bak are activated and oligomerize during apoptosis. Cell Death Differ 21:196–205. https://doi.org/10.1038/cdd.2013.139.
28. Escudero S, Zaganjor E, Lee S, Mill CP, Morgan AM, Crawford EB, Chen JH, Wales TE, Mourtada R, Luccarelli J, Bird GH, Steidl U, Engen JR, Haigis MC, Opferman JT, Walensky LD. 2018. Dynamic regulation of long-chain fatty acid oxidation by a noncanonical interaction between the MCL-1 BH3 helix and VLCAD. Mol Cell 69:729–743.e7. https://doi.org/10.1016/j.molcel.2018.02.005.
29. Perciavalle RM, Stewart DP, Koss B, Lynch J, Milasta S, Bathina M, Temirov J, Cleland MM, Pelletier S, Schuetz JD, Youle RJ, Green DR, Opferman JT. 2012. Anti-apoptotic MCL-1 localizes to the mitochondrial matrix and couples mitochondrial fusion to respiration. Nat Cell Biol 14:575–583. https://doi.org/10.1038/ncb2488.
30. Germain M, Nguyen AP, Le Grand JN, Arbour N, Vanderluit JL, Park DS, Opferman JT, Slack RS. 2011. MCL-1 is a stress sensor that regulates autophagy in a developmentally regulated manner. EMBO J 30:395–407. https://doi.org/10.1038/emboj.2010.327.
31. Quentmeier H, Geffers R, Hauer V, Nagel S, Pommerenke C, Uphoff CC, Zaborski M, Drexler HG. 2022. Inhibition of MCL1 induces apoptosis in anaplastic large cell lymphoma and in primary effusion lymphoma. Sci Rep 12:1085. https://doi.org/10.1038/s41598-022-04916-6.
32. Kotschy A, Szlavik Z, Murray J, Davidson J, Maragno AL, Le Toumelin-Braizat G, Chanrion M, Kelly GL, Gong JN, Moujalled DM, Bruno A, Csekei M, Paczal A, Szabo ZB, Sipos S, Radics G, Proszenyak A, Balint B, Ondi L, Blasko G, Robertson A, Surgenor A, Dokurno P, Chen I, Matassova N, Smith J, Pedder C, Graham C, Studeny A, Lysiak-Auvity G, Girard AM, Grave F, Segal D, Riffkin CD, Pomilio G, Galbraith LC, Aubrey BJ, Brennan MS, Herold MJ, Chang C, Guasconi G, Cauquil N, Melchiore F, Guigal-Stephan N, Lockhart B, Colland F, Hickman JA, Roberts AW, Huang DC, Wei AH, et al. 2016. The MCL1 inhibitor S63845 is tolerable and effective in diverse cancer models. Nature 538:477–482. https://doi.org/10.1038/nature19830.
33. Pelossof R, Fairchild L, Huang CH, Widmer C, Sreedharan VT, Sinha N, Lai DY, Guan Y, Premsrirut PK, Tschaharganeh DF, Hoffmann T, Thapar V, Xiang Q, Garippa RJ, Ratsch G, Zuber J, Lowe SW, Leslie CS, Fellmann C. 2017. Prediction of potent shRNAs with a sequential classification algorithm. Nat Biotechnol 35:350–353. https://doi.org/10.1038/nbt.3807.
34. van der Meer D, Barthorpe S, Yang W, Lightfoot H, Hall C, Gilbert J, Francies HE, Garnett MJ. 2019. Cell Model Passports—a hub for clinical, genetic and functional datasets of preclinical cancer models. Nucleic Acids Res 47:D923–D929. https://doi.org/10.1093/nar/gky872.
35. Sarid R, Sato T, Bohenzky RA, Russo JJ, Chang Y. 1997. Kaposi's sarcoma-associated herpesvirus encodes a functional bcl-2 homologue. Nat Med 3:293–298. https://doi.org/10.1038/nm0397-293.
36. Cheng EH, Nicholas J, Bellows DS, Hayward GS, Guo HG, Reitz MS, Hardwick JM. 1997. A Bcl-2 homolog encoded by Kaposi sarcoma-associated virus, human herpesvirus 8, inhibits apoptosis but does not heterodimerize with Bax or Bak. Proc Natl Acad Sci U S A 94:690–694. https://doi.org/10.1073/pnas.94.2.690.
37. Tsherniak A, Vazquez F, Montgomery PG, Weir BA, Kryukov G, Cowley GS, Gill S, Harrington WF, Pantel S, Krill-Burger JM, Meyers RM, Ali L, Goodale A, Lee Y, Jiang G, Hsiao J, Gerath WFJ, Howell S, Merkel E, Ghandi M, Garraway LA, Root DE, Golub TR, Boehm JS, Hahn WC. 2017. Defining a cancer dependency map. Cell 170:564–576.e16. https://doi.org/10.1016/j.cell.2017.06.010.
38. Vikstrom I, Carotta S, Luthje K, Peperzak V, Jost PJ, Glaser S, Busslinger M, Bouillet P, Strasser A, Nutt SL, Tarlinton DM. 2010. Mcl-1 is essential for

germinal center formation and B cell memory. Science 330:1095–1099. https://doi.org/10.1126/science.1191793.
39. Peperzak V, Vikstrom I, Walker J, Glaser SP, LePage M, Coquery CM, Erickson LD, Fairfax K, Mackay F, Strasser A, Nutt SL, Tarlinton DM. 2013. Mcl-1 is essential for the survival of plasma cells. Nat Immunol 14:290–297. https://doi.org/10.1038/ni.2527.
40. Carrington EM, Vikstrom IB, Light A, Sutherland RM, Londrigan SL, Mason KD, Huang DC, Lew AM, Tarlinton DM. 2010. BH3 mimetics antagonizing restricted prosurvival Bcl-2 proteins represent another class of selective immune modulatory drugs. Proc Natl Acad Sci U S A 107:10967–10971. https://doi.org/10.1073/pnas.1005256107.
41. Robinson MJ, Webster RH, Tarlinton DM. 2020. How intrinsic and extrinsic regulators of plasma cell survival might intersect for durable humoral immunity. Immunol Rev 296:87–103. https://doi.org/10.1111/imr.12895.
42. Wang C, Zhang L, Ke L, Ding W, Jiang S, Li D, Narita Y, Hou I, Liang J, Li S, Xiao H, Gottwein E, Kaye KM, Teng M, Zhao B. 2020. Primary effusion lymphoma enhancer connectome links super-enhancers to dependency factors. Nat Commun 11:6318. https://doi.org/10.1038/s41467-020-20136-w.
43. Park A, Oh S, Jung KL, Choi UY, Lee HR, Rosenfeld MG, Jung JU. 2020. Global epigenomic analysis of KSHV-infected primary effusion lymphoma identifies functional MYC superenhancers and enhancer RNAs. Proc Natl Acad Sci U S A 117:21618–21627. https://doi.org/10.1073/pnas.1922216117.
44. Lam WY, Bhattacharya D. 2018. Metabolic links between plasma cell survival, secretion, and stress. Trends Immunol 39:19–27. https://doi.org/10.1016/j.it.2017.08.007.
45. Wiest DL, Burkhardt JK, Hester S, Hortsch M, Meyer DI, Argon Y. 1990. Membrane biogenesis during B cell differentiation: most endoplasmic reticulum proteins are expressed coordinately. J Cell Biol 110:1501–1511. https://doi.org/10.1083/jcb.110.5.1501.
46. Tellier J, Shi W, Minnich M, Liao Y, Crawford S, Smyth GK, Kallies A, Busslinger M, Nutt SL. 2016. Blimp-1 controls plasma cell function through the regulation of immunoglobulin secretion and the unfolded protein response. Nat Immunol 17:323–330. https://doi.org/10.1038/ni.3348.
47. McBrayer SK, Cheng JC, Singhal S, Krett NL, Rosen ST, Shanmugam M. 2012. Multiple myeloma exhibits novel dependence on GLUT4, GLUT8, and GLUT11: implications for glucose transporter-directed therapy. Blood 119:4686–4697. https://doi.org/10.1182/blood-2011-09-377846.
48. Kuehnle N, Manzano M, Gottwein E. 2022. Cellular FLIP protects KSHV-transformed lymphoma cells from TRAIL-independent TRAIL receptor 1-mediated cell death. bioRxiv. https://doi.org/10.1101/2022.08.17.504167.
49. De Leo A, Chen HS, Hu CC, Lieberman PM. 2017. Deregulation of KSHV latency conformation by ER-stress and caspase-dependent RAD21-cleavage. PLoS Pathog 13:e1006596. https://doi.org/10.1371/journal.ppat.1006596.
50. Johnston BP, Pringle ES, McCormick C. 2019. KSHV activates unfolded protein response sensors but suppresses downstream transcriptional responses to support lytic replication. PLoS Pathog 15:e1008185. https://doi.org/10.1371/journal.ppat.1008185.
51. Kim YJ, Kim Y, Kumar A, Kim CW, Toth Z, Cho NH, Lee HR. 2021. Kaposi's sarcoma-associated herpesvirus latency-associated nuclear antigen dysregulates expression of MCL-1 by targeting FBW7. PLoS Pathog 17:e1009179. https://doi.org/10.1371/journal.ppat.1009179.
52. Wang HW, Trotter MW, Lagos D, Bourboulia D, Henderson S, Makinen T, Elliman S, Flanagan AM, Alitalo K, Boshoff C. 2004. Kaposi sarcoma herpesvirus-induced cellular reprogramming contributes to the lymphatic endothelial gene expression in Kaposi sarcoma. Nat Genet 36:687–693. https://doi.org/10.1038/ng1384.
53. Diepstraten ST, Anderson MA, Czabotar PE, Lessene G, Strasser A, Kelly GL. 2022. The manipulation of apoptosis for cancer therapy using BH3-mimetic drugs. Nat Rev Cancer 22:45–64. https://doi.org/10.1038/s41568-021-00407-4.
54. Roberts AW, Davids MS, Pagel JM, Kahl BS, Puvvada SD, Gerecitano JF, Kipps TJ, Anderson MA, Brown JR, Gressick L, Wong S, Dunbar M, Zhu M, Desai MB, Cerri E, Heitner Enschede S, Humerickhouse RA, Wierda WG, Seymour JF. 2016. Targeting BCL2 with venetoclax in relapsed chronic lymphocytic leukemia. N Engl J Med 374:311–322. https://doi.org/10.1056/NEJMoa1513257.
55. Davids MS, Roberts AW, Seymour JF, Pagel JM, Kahl BS, Wierda WG, Puvvada S, Kipps TJ, Anderson MA, Salem AH, Dunbar M, Zhu M, Peale F, Ross JA, Gressick L, Desai M, Kim SY, Verdugo M, Humerickhouse RA, Gordon GB, Gerecitano JF. 2017. Phase I first-in-human study of venetoclax in patients with relapsed or refractory non-Hodgkin lymphoma. J Clin Oncol 35:826–833. https://doi.org/10.1200/JCO.2016.70.4320.
56. Davids MS, Roberts AW, Kenkre VP, Wierda WG, Kumar A, Kipps TJ, Boyer M, Salem AH, Pesko JC, Arzt JA, Mantas M, Kim SY, Seymour JF. 2021. Long-term follow-up of patients with relapsed or refractory non-Hodgkin lymphoma treated with venetoclax in a phase I, first-in-human study. Clin Cancer Res 27:4690–4695. https://doi.org/10.1158/1078-0432.CCR-20-4842.
57. Konopleva M, Pollyea DA, Potluri J, Chyla B, Hogdal L, Busman T, McKeegan E, Salem AH, Zhu M, Ricker JL, Blum W, DiNardo CD, Kadia T, Dunbar M, Kirby R, Falotico N, Leverson J, Humerickhouse R, Mabry M, Stone R, Kantarjian H, Letai A. 2016. Efficacy and biological correlates of response in a phase II Study of venetoclax monotherapy in patients with acute myelogenous leukemia. Cancer Discov 6:1106–1117. https://doi.org/10.1158/2159-8290.CD-16-0313.
58. Castaneda AF, Glaunsinger BA. 2019. The interaction between ORF18 and ORF30 is required for late gene expression in Kaposi's sarcoma-associated herpesvirus. J Virol 93:e01488-18. https://doi.org/10.1128/JVI.01488-18.
59. Upreti M, Chu R, Galitovskaya E, Smart SK, Chambers TC. 2008. Key role for Bak activation and Bak-Bax interaction in the apoptotic response to vinblastine. Mol Cancer Ther 7:2224–2232. https://doi.org/10.1158/1535-7163.MCT-07-2299.
60. Seiler CY, Park JG, Sharma A, Hunter P, Surapaneni P, Sedillo C, Field J, Algar R, Price A, Steel J, Throop A, Fiacco M, LaBaer J. 2014. DNASU plasmid and PSI:Biology-Materials repositories: resources to accelerate biological research. Nucleic Acids Res 42:D1253–D1260. https://doi.org/10.1093/nar/gkt1060.
61. Doench JG, Fusi N, Sullender M, Hegde M, Vaimberg EW, Donovan KF, Smith I, Tothova Z, Wilen C, Orchard R, Virgin HW, Listgarten J, Root DE. 2016. Optimized sgRNA design to maximize activity and minimize off-target effects of CRISPR-Cas9. Nat Biotechnol 34:184–191. https://doi.org/10.1038/nbt.3437.
62. Ran FA, Hsu PD, Wright J, Agarwala V, Scott DA, Zhang F. 2013. Genome engineering using the CRISPR-Cas9 system. Nat Protoc 8:2281–2308. https://doi.org/10.1038/nprot.2013.143.